Mon. Not. R. Astron. Soc. **000**, 000–000 (0000) Printed 5 February 2008 (MN LaTeX style file v2.2)

arXiv:astro-ph/0602306v1 14 Feb 2006

The evolution of misaligned accretion discs and spinning black holes

G. Lodato and J. E. Pringle
Institute of Astronomy, Madingley Road, Cambridge, CB3 0HA

5 February 2008

ABSTRACT

In this paper we consider the process of alignment of a spinning black hole and a surrounding misaligned accretion disc. We use a simplified set of equations, that describe the evolution of the system in the case where the propagation of warping disturbances in the accretion disc occurs diffusively, a situation likely to be common in the thin discs in Active Galactic Nuclei (AGN). We also allow the direction of the hole spin to move under the action of the disc torques. In such a way, the evolution of the hole-disc system is computed self-consistently. We consider a number of different situations and we explore the relevant parameter range, by varying the location of the warp radius $R_{\rm w}$ and the propagation speed of the warp. We find that the dissipation associated with the twisting of the disc results in a large increase in the accretion rate through the disc, so that AGN accreting from a misaligned disc are likely to be significantly more luminous than those accreting from a flat disc. We compute explicitly the time-scales for the warping of the disc and for the alignment process and compare our results with earlier estimates based on simplified steady-state solutions. We also confirm earlier predictions that, under appropriate circumstances, accretion can proceed in a counter-aligned fashion, so that the accreted material will spin-down the hole, rather than spinning it up. Our results have implication in a number of different observational features of AGN such as the orientation and shape of jets, the shape of X-ray iron lines, and the possibility of obscuration and absorption of X-ray by the outer disc as well as the general issue of the spin history of black holes during their growth.

Key words: accretion, accretion discs – black hole physics – galaxies: active – galaxies: nuclei

1 INTRODUCTION

There are strong observational and theoretical grounds for believing that accretion discs around black holes may be twisted or warped, in the sense that the plane of the Keplerian orbits varies continuously with radius and with time. From the observational point of view, warped discs have been observed in the nuclei of active galaxies (AGN) at relatively large distances from the central supermassive black hole ($\sim$ 1 pc), especially though water maser observation (for example: in NGC4258, Herrnstein et al. 1996, or in Circinus, Greenhill et al. 2003). A warped inner accretion disc might also be the explanation of the apparent lack of correlation between the direction of the radio jets emanating from AGN and the plane of the host galaxy disc (Kinney et al. 2000; Schmitt et al. 2002). Modelling of accretion events onto the cores of galaxies seems to indicate that they occur at random orientations (Kendall et al. 2003; Saitoh & Wada 2004). In addition, a warp in the disc might lead to interesting phenomena of obscuration of the central engine in an AGN (Phinney 1989; Greenhill et al. 2003; Nayakshin 2005).

From a theoretical perspective, there are a number of possible physical mechanisms that can cause the disc to be warped. On the large scale, a warp might be produced through the interaction of the disc with a smaller mass companion orbiting in an inclined orbit. However, closer to the black hole, at distances of the order of $\approx 10^2-10^3 R_{\rm S}$, where $R_{\rm S}$ is the Schwarzschild radius of the black hole, the most likely cause of warping is due to relativistic effects. In particular, if the black hole is spinning and the spin axis of the hole is misaligned with the axis of rotation of the disc (or, equivalently, if the hole's angular momentum is misaligned with respect to the angular momentum of the accreting matter), then the Lense-Thirring precession produces a warp in the disc. This process is called the Bardeen-Petterson effect

(Bardeen & Petterson 1975). Since the rate of the Lense-Thirring precession is a strong function of radius $\propto R^{-3}$, the general result is that the inner parts of the disc tends to align the direction (but not necessarily the sense, see below) of its specific angular momentum with that of the hole, while outside a typical radius, the warp radius, $R_{\rm w} \approx 10^2 R_{\rm S}$ (Natarajan & Pringle 1998; King et al. 2005), the disc tends to retain its original direction of rotation.

In this paper, we explore the time-dependent evolution of the process of alignment between an accretion disc and a spinning black hole. We consider the case where the propagation of the warp occurs diffusively. This occurs (Papaloizou & Pringle 1983) when the dimensionless viscosity coefficient in the disc (here called α_1, see below) is larger than the disc aspect ratio H/R (which should be the case for typical AGN discs, Wijers & Pringle 1999). Here we are not concerned with the detailed physical mechanism responsible for the propagation of the warp, the discussion of which would require large 3D numerical simulations (c.f. Nelson & Papaloizou 2000; Fragile & Anninos 2005). Rather, we explore here the long term evolution of the system by using a simplified 1D approach (Pringle 1992). Additionally, in our implementation, we allow the black hole spin direction to evolve as a consequence of the mutual torques with the hole. In this way, the evolution of the hole spin and the warping of the disc, which might occur on similar time-scales, are computed simultaneously and self-consistently. We explicitly evaluate the above-mentioned time-scales, and we also determine the effect that the warping process has on the accretion phenomenon. In particular, we find that the additional dissipation associated with the twisting of the disc leads to a large enhancement in the accretion rate (up to a factor ~ 10).

We also address the issue of whether the disc and the hole angular momenta might end up being counter-aligned. This possibility appeared ruled out by the analysis of Scheuer & Feiler (1996) (hereafter SF). However, King et al. (2005) have recently challenged this conclusion, and, using simple geometrical arguments, find that counter-alignment should take place when the magnitude of the hole angular momentum $J_{\rm h}$, the disc angular momentum $J_{\rm d}$ and their initial misalignment are in the following relation:

$$\frac{J_{\rm d}}{J_{\rm h}} < -2\cos\theta, \qquad (1)$$

where θ is the initial angle between the two angular momenta. King et al. (2005) argue that SF did not find counter-alignment because they implicitly assume that $J_{\rm d}$ was infinitely large, therefore making inequality (1) impossible to be satisfied. Here, we re-examine this issue by performing a number of simulations with given $J_{\rm d}$ and $J_{\rm h}$ and conclude that indeed counter-alignment is possible when inequality (1) is satisfied. When counter-alignment occurs, accretion of matter onto the hole causes the hole to spin-down, rather than spin-up. The possibility of counter-alignment is therefore particularly relevant to the description of the spin history of black holes (Volonteri et al. 2005) and to the determination of the innermost stable orbit, which in turn determines the efficiency of conversion of matter into luminosity.

The paper is organized as follows. In Section 2 we describe the basic set of equations that we use to determine the evolution of the accretion disc and of the spinning black hole. In Section 3 we examine more thoroughly the steady-state equations found by SF, discussing their applicability and their limitations. In Section 4 we perform a number of simulations describing the evolution of “warped spreading rings”, where we consider the evolution of thin rings of matter, initially inclined with respect to the hole spin direction, as they are accreted and twisted by the black hole. In Section 5 we discuss our results and draw our conclusions

2 BASIC EQUATIONS

In this Section we briefly describe the model that we use to follow the evolution of the system. We consider a system comprising a black hole at $R = 0$ (note that here R is a purely spherical coordinate and not the cylindrical radius), with spin angular momentum $\mathbf{J}_{\rm h}$, surrounded by a disc, with surface density Σ and specific angular momentum density $\mathbf{L}(R)$, in Keplerian rotation around the black hole. Since we expect the interesting disc dynamics to occur in the region of the warp radius $R_{\rm w} \gg R_{\rm S}$, treating the black hole as a point mass and using Newtonian dynamics is adequate for our present purposes. The modulus of the specific angular momentum density is thus given by $L(R) = \Sigma\sqrt{GMR}$, where M is the mass of the black hole. The unit vector indicating the local direction of the specific angular momentum in the disc is denoted by $\mathbf{l}(R)$. We further denote by $\mathbf{J}_{\rm d}$ the total angular momentum of the disc:

$$\mathbf{J}_{\rm d} = \int 2\pi R\mathbf{L}(R){\rm d}R \qquad (2)$$

We follow the formalism of Pringle (1992) and introduce the two viscosities ν_1 and ν_2, where ν_1 is the standard shear viscosity in a flat disc, and ν_2 is the viscosity associated with vertical shear motions and which describes the diffusion of warping disturbances through the disc. The equation of motion for the specific angular momentum in the disc is (Pringle 1992):

$$\begin{aligned}\frac{\partial \mathbf{L}}{\partial t} = \quad & \frac{3}{R}\frac{\partial}{\partial R}\left[\frac{R^{1/2}}{\Sigma}\frac{\partial}{\partial R}(\nu_1\Sigma R^{1/2})\mathbf{L}\right] \\ + \quad & \frac{1}{R}\frac{\partial}{\partial R}\left[\left(\nu_2 R^2\left|\frac{\partial \mathbf{l}}{\partial R}\right|^2 - \frac{3}{2}\nu_1\right)\mathbf{L}\right] \qquad (3) \\ + \quad & \frac{1}{R}\frac{\partial}{\partial R}\left(\frac{1}{2}\nu_2 R|\mathbf{L}|\frac{\partial \mathbf{l}}{\partial R}\right).\end{aligned}$$

Note that the above equation is a generalization of the standard accretion disc equation (e.g. Pringle 1981) and reduces to it in the case of a flat disc ($\partial\mathbf{l}/\partial R = 0$). The viscosity coefficients ν_1 and ν_2, of course, are in general a function of local disc properites as well as of R. However, in the rest of the paper, we will explore the simple case where both ν_1 and ν_2 are constants, independent on R. Papaloizou & Pringle (1983) have shown that in the linear approximation corresponding to small warp angles they are related through $\nu_2/\nu_1 = 1/2\alpha_1^2$, where α_1 is the standard α parameter associated with the viscosity ν_1 (Shakura & Sunyaev 1973). In this picture, therefore, the stress associated with warp propagation is much larger than the viscous stress, since α_1 is generally much smaller than unity. However, the actual value of ν_2 in the non-linear case has still to be determined (see discussion in Section 2.1. below).

Equation (3) describes the evolution of a warped disc subject only to internal torques. In order to study the Bardeen-Petterson effect we add a term on the right-hand side of equation (3), that describes the relative torque between the disc and the hole due to Lense-Thirring precession:

$$\left.\frac{\partial \mathbf{L}}{\partial t}\right|_{\rm LT} = \mathbf{\Omega}_{\rm p} \times \mathbf{L}, \tag{4}$$

where the precession rate $\mathbf{\Omega}_{\rm p}$ is given by (e.g. Kumar & Pringle 1985) $\mathbf{\Omega}_{\rm p} = \boldsymbol{\omega}_{\rm p}/R^3$, with:

$$\boldsymbol{\omega}_{\rm p} = \frac{2G\mathbf{J}_{\rm h}}{c^2}, \tag{5}$$

where c is the speed of light. This is valid for $R \gg R_{\rm S}$.

In most of our simulations, we also allow the black hole spin to evolve as a consequence of the torques exerted by the disc. The equation of motion for the hole spin follows directly from Newton's third law and we have:

$$\frac{{\rm d}\mathbf{J}_{\rm h}}{{\rm d}t} = -2\pi \int \mathbf{\Omega}_{\rm p} \times \mathbf{L} R {\rm d}R, \tag{6}$$

where the integral is taken over the disc surface. Note that, since the torque on the black hole is perpendicular to the hole angular momentum, the modulus of $\mathbf{J}_{\rm h}$ is constant with time. The only effects of the relative torques are to make the hole spin change direction or precess and affect alignment with the angular momentum of the disc. The calculations here neglect the changes in the magnitude of the spin of the hole caused by the accretion of matter onto it. In general we expect the accretion induced change in the hole spin to occur on a longer time-scale than the disc induced change in spin direction both because of the lever-arm effect at $R_{\rm w}$ (Rees 1978; Natarajan & Pringle 1998) and because warp propagation (ν_2) typically occurs faster than mass propagation (ν_1). We discuss this issue more in detail below.

We solve equations (3) and (6) numerically using the scheme described in Pringle (1992). We employ a logarithmically spaced radial grid spanning three to four orders of magnitude for most simulations. Equation (6) is solved using a standard fourth-order Runge-Kutta method.

2.1 Validity of our approach and theoretical uncertainties

Our basic evolutionary equation [Equation (3)] assumes that the evolution of the disc warp is diffusive and the response of the disc to the warping perturbation is completely determined, in our approach, by the coefficient ν_2. The basic motivation for our assumption stems in the analysis of Papaloizou & Pringle (1983), who have shown that the warp propagation is indeed diffusive (as long as $\alpha > H/R$) in the linear regime, and assuming that the internal disc motions are purely hydrodynamic, and that the viscosity present is the standard Navier-Stokes viscosity. As mentioned above, Papaloizou & Pringle (1983) also find that $\nu_2/\nu_1 = 1/2\alpha_1^2$, which is generally much larger than unity.

In fact, even with these simplifying assumptions, the linear, hydrodynamic analysis predicts the presence of precessional terms (Papaloizou & Pringle 1983; Ogilvie 2000). These are however second order terms and we neglect them here.

However, the behaviour of real discs is surely more complex than what is described simply by Equation (3). Turbulence is likely to be controlled by magnetic fields (Balbus & Hawley 1998), and what kind of viscosity arises under these conditions is yet to be fully determined. The only attempt at measuring ν_2 in the presence of MHD turbulence has been done by Torkelsson et al. (2000), who find, within the limitations of a shearing box approximation, that also in this case one should expect ν_2/ν_1 to be relatively large.

Additionally, non-linear effects are going to be important (indeed, as described below, most of our simulations deal with non-linear warps). The behaviour of the disc in such regimes is much harder to describe. The only analytical theories of non-linear warps are by Ogilvie (1999, 2000) and Ogilvie & Dubus (2001). These are for purely hydrodynamic discs and they generally assume a polytropic equation of state. In addition, such analyses are limited to mildly non-linear warps and the resulting non-linear corrections are dependent on the detailed disc structure ($\Sigma(R)$, $H(R)$, ...). In particular, Ogilvie (1999) has shown that the first non-linear corrections to the diffusion coefficients become important when the amplitude of the warp $\psi = R|\partial \mathbf{l}/\partial R| \gtrsim \alpha$. For these amplitudes, the horizontal shear motions induced by the warp become supersonic, inducing shocks and additional dissipation in the disc, not included in Ogilvie (1999). In the presence of very large warps there is also the possibility (Gammie et al. 2000) of additional dissipation caused by fluid instabilities. In this case, one possibility is that the ratio ν_2/ν_1 might be substantially reduced.

In view of all the above uncertainties, we have opted for a straightforward, and somewhat abstract, approach. The reason for doing so is that it keeps the physical processes involved simple, and does not specialize to any particular disc application (such as AGN, X-ray binaries, etc.). This enables a basic understanding of the physics involved in the alignment (or possibly counter-alignment, see below) process, without adding physically uncertain, and likely unnecessary, complications.

We have therefore adopted the simple approach of Equation (3), but allowing the main parameter ν_2/ν_1 to lie within a large range of values (from very large values, as expected from the linear analysis, to smaller values, perhaps ≈ 1, that might arise in strongly non-linear conditions), determining in this way the dependence of the alignment process on this basic unknown parameter.

More complex numerical simulations will be needed to determine the local response of a thin disc in strongly non-linear conditions, but we leave this for future analyses. We expect that the behaviour determined here will qualitatively describe the disc evolution (using the appropriate values of the diffusion coefficient) even in strongly non-linear regimes.

3 STEADY-STATE SOLUTIONS

SF have found analytical steady-state solutions to equation (3), in the presence of the forced precession for small tilt angles described in equation (4), subject to various simplifying assumptions about the disc density distribution and

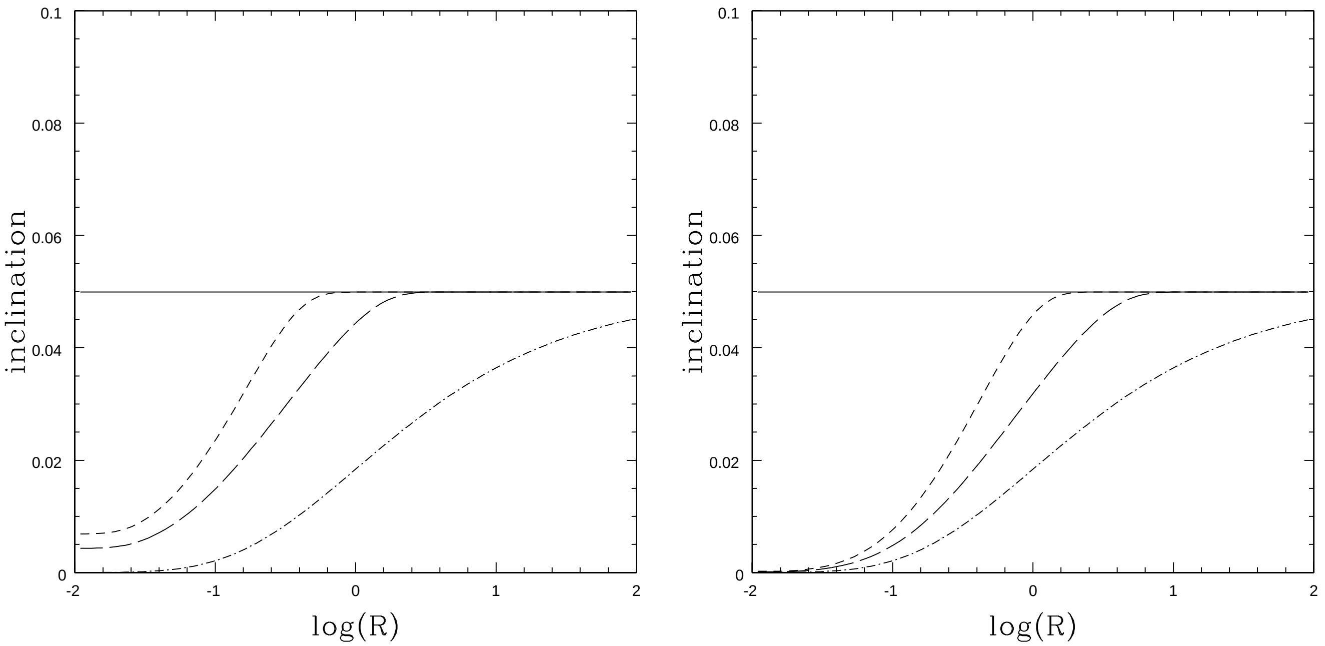

Figure 1. Evolution of the warp in the case where $R_{\rm w} = \omega_{\rm p}/\nu_1 = 0.25$ ($\log R_{\rm w} = -0.6$) and $\nu_2/\nu_1 = 1$ (left panel) and $\nu_2/\nu_1 = 10$ (right panel). The lines refer to $t = 0$ (solid line), $t = 0.05$ (short-dashed line) and $t = 1$ (long-dashed line), where the times are expressed in units of the viscous time (R^2/ν_1) at $R = 1$. The dot-dashed line shows the SF solution in this case. At time t, the warped portion of the disc extends out to a radius such that $t \approx R^2/\nu_2$, showing that the warp indeed diffuses out at this time-scale.

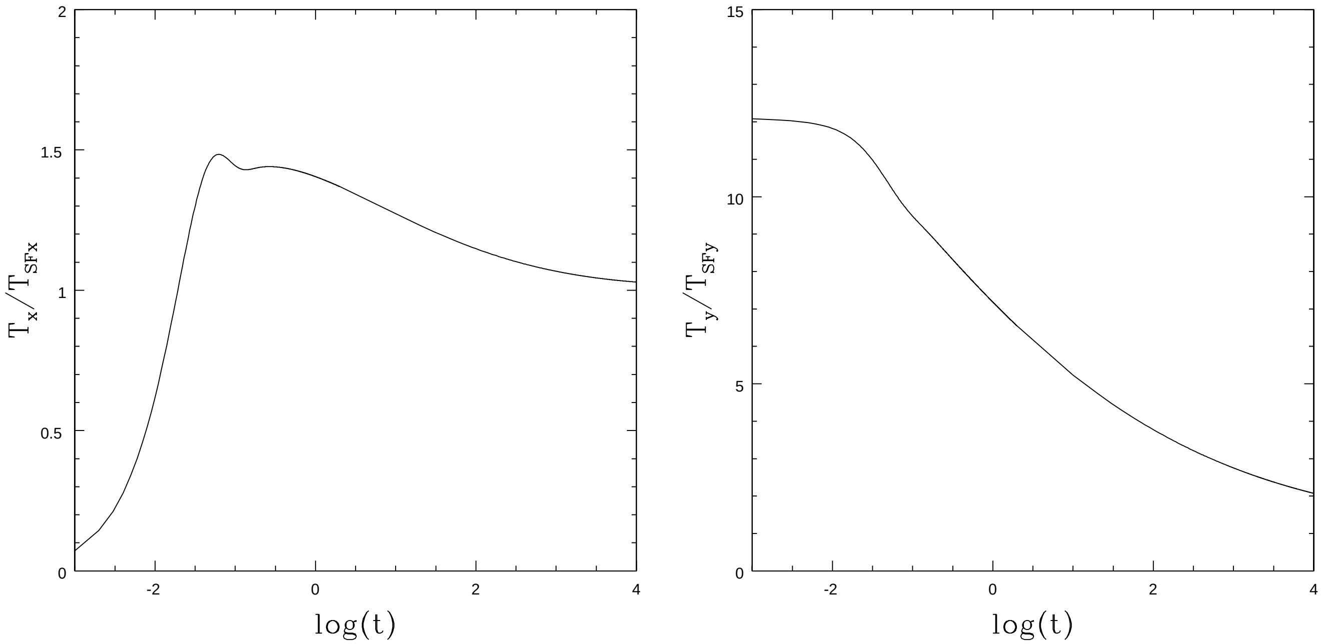

Figure 2. Evolution of the the x- (left panel) and y-component (right panel) of the torque exerted by the disc on the hole, normalized to their asymptotic values in a steady state, in the case where $\nu_2/\nu_1 = 10$. The x-component, responsible for the alignment of the hole, is never very far from the asymptotic value, except in the very early stages of the evolution. On the other hand, the y-component, responsible for the precession of the hole's spin can be significantly different and approaches the steady state value more slowly.

the inner boundary. The steady-state warp only depends on a single parameter $R_\mathrm{w} = \omega_\mathrm{p}/\nu_2$, the warp radius, which is the radius at which the warp propagation time-scale equals the local forced precession rate. Roughly speaking, the disc becomes aligned with the hole spin at $R \ll R_\mathrm{w}$ and keeps its original inclination for $R \gg R_\mathrm{w}$. The SF solution takes a very compact form in terms of the complex variable $W = l_x + il_y$, where l_x and l_y are the x and y component of the unit vector parallel to the local direction of the disc's specific angular momentum, and the z-axis is parallel to the black hole spin. In terms of W, the SF solution reads:

$$W = K \exp\left[-2(1-i)\left(\frac{R_\mathrm{w}}{R}\right)^{1/2}\right], \qquad (7)$$

where K is a complex constant that determines the amplitude of the warp at large radii. This solution is inaccurate at very small radii, close to the black hole, and holds only under the assumption that the inner disc radius $R_\mathrm{in} \ll R_\mathrm{w}$ and $K \ll 1$.

Then, SF compute the torque exerted by the steady state disc on the black hole and are therefore able to compute the time-scale over which the hole eventually aligns with the outer disc. The surface density distribution and the radial profile of the warp are assumed to correspond to that of a steadily accreting disc and thus this procedure implicitly assumes that the alignment time-scale is much longer than the warp propagation time-scale (over which the steady state solution is attained). The alignment time-scale is roughly given by:

$$t_\mathrm{align} \sim \frac{J_\mathrm{h}}{J_\mathrm{d}(R_\mathrm{w})}\frac{R_\mathrm{w}^2}{\nu_2}, \qquad (8)$$

where here $J_\mathrm{d}(R_\mathrm{w})$ is the angular momentum of the disc within the warp radius. The time-scale computed by SF is therefore formally valid only if the angular momentum of the hole is much larger than the angular momentum of the disc within the warp radius. In the steady-state computed by SF, it can be easily shown that:

$$t_\mathrm{align} = 3a\frac{\nu_1}{\nu_2}\frac{M}{\dot{M}}\left(\frac{R_\mathrm{s}}{R_\mathrm{w}}\right)^{1/2}, \qquad (9)$$

where a is the spin parameter of the hole, R_s is its Schwarzschild radius and $\dot{M}$ is the steady state accretion rate.

A second limitation of the SF solution, as pointed out by King et al. (2005) (see also Introduction), is that their steady-state disc formally extends to infinity and therefore has an infinite total angular momentum. According to King et al. (2005), this prevents the possibility of obtaining a configuration where eventually the disc and the hole angular momenta end up being counter-aligned.

With the above discussion in mind, we now assess the validity of the SF solution by computing explicitly the evolution of an initially flat but tilted disc and following its approach to a steady state. In this case, we will keep the hole spin direction fixed. The disc extends from $R_\mathrm{in} = 10^{-2}$ to $R_\mathrm{out} = 10^2$. Particular care has been given to the boundary conditions. In fact, we would like to have a numerical scheme that conserves angular momentum as far as possible. In order to do this, we implement the boundary conditions exactly as described in Pringle (1992), in such a way that at both the inner and outer boundary no torque is provided to the disc in either the azimuthal or the tilt direction (apart from the Lense-Thirring torques). Note that the usual inner boundary condition adopted in numerical models of accretion discs (i.e. $\Sigma = 0$, see, for example, Pringle et al. 1986), implies a zero *viscous* torque at the inner edge, thus implying an advective loss of angular momentum from the inner edge and consequently allowing accretion. In our implementation, in order to produce an accreting, but torque-free inner boundary, we set up a sink of material there. In effect, we add a term on the right-and side of Equation (3) of the form:

$$\left.\frac{\partial \mathbf{L}}{\partial t}\right|_\mathrm{in} = -\frac{\mathbf{L}f(R)}{t_\mathrm{sink}}, \qquad (10)$$

where $f(R)$ is a dimensionless function strongly peaked at the inner edge and t_sink is an adjustable time-scale, chosen to be small enough to approximate the usual $\Sigma = 0$ inner boundary condition.

We feed the disc at a constant mass accretion rate $\dot{M} = 1$ between $R = 70$ and $R = 90$, with a flat spatial distribution. Time units are determined by setting $\nu_1 = 1$. The initial surface density of the disc is taken to be that appropriate to a steady state for a flat disc in this configuration:

$$\begin{aligned}\Sigma_0 \;=\; & (R^{1/2} - R_\mathrm{in}^{1/2})/3\pi R^{1/2} \qquad R_\mathrm{in} < R < R_\mathrm{add} \\ & (R_\mathrm{add}^{1/2} - R_\mathrm{in}^{1/2})/3\pi R^{1/2} \qquad R_\mathrm{add} < R < R_\mathrm{out},\end{aligned} \qquad (11)$$

where $R_\mathrm{add} = 80$ is the mean radius at which we add matter. The disc is initially flat, and inclined with respect to the hole spin by an angle θ. The amplitude of the warp is thus given by $K = \sin\theta$. Before running the simulations, we have checked that, in the absence of Lense-Thirring precession, the disc is indeed in a steady state.

In this case (where the hole spin is kept fixed), the system only depends on the two parameters ν_2/ν_1 and R_w. Below we discuss separately the two cases where $R_\mathrm{w} \gg R_\mathrm{in}$ and where $R_\mathrm{w} \approx R_\mathrm{in}$. Note that we therefore assume that $R_\mathrm{in} \gg R_\mathrm{S}$.

3.1 Large warp radius

In this Section we describe the evolution of the system with a relatively large warp radius (with respect to the inner disc radius) $R_\mathrm{w} = \omega_\mathrm{p}/\nu_2 = 0.25 = 25R_\mathrm{in}$. The initial inclination angle between the disc and the hole was here taken to be $\theta = 0.05$. In Fig. 1 we show the evolution of the local inclination between the disc and the hole at different times for the two cases where $\nu_2/\nu_1 = 1$ (left panel) and $\nu_2/\nu_1 = 10$ (right panel). The lines refer to $t = 0$ (solid line), $t = 0.05$ (short-dashed line) and $t = 1$ (long-dashed line), where the times are expressed in units of the viscous time (R^2/ν_1) at $R = 1$. The dot-dashed line shows the SF solution in this case. As expected, in the case where $\nu_2/\nu_1 = 10$ the propagation of the warp is much faster so that, at any given time, a larger portion of the disc is warped in this case with respect to the case where $\nu_2/\nu_1 = 1$. Plotting the same quantity as in Fig. 1, but where the two simulations are portrayed at the same time in units of R^2/ν_2 (the warp diffusion time-scale), evaluated at $R = 1$, shows that, in this time units,

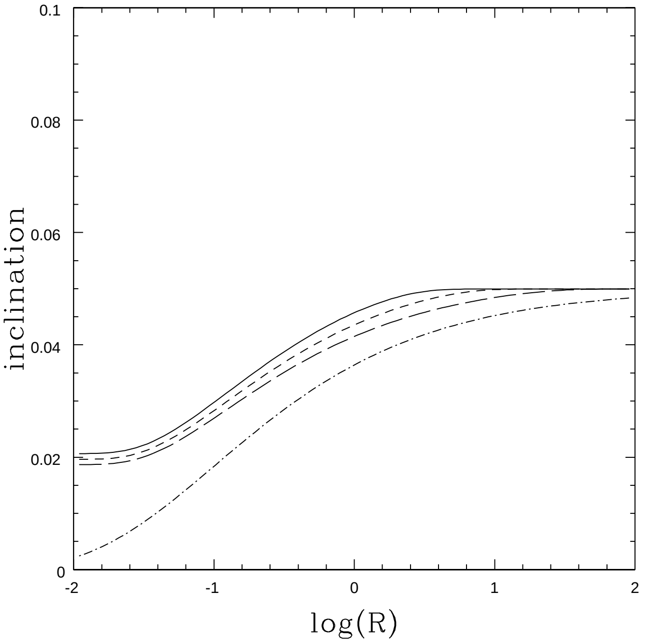

Figure 3. Relative inclination between the disc and the hole at $t = 0.5$ (solid line), $t = 3$ (short-dashed line) and at $t = 60$ (long-dashed line). The steady-state solution in this case is significantly different than what predicted by SF (dot-dashed line). Here $R_{\rm w} = 0.025$ ($\log R_{\rm w} = -1.6$).

the warped portion of the disc expands at the same rate in the two cases.

An interesting feature that can be seen from Fig. 1 is that in the small ν_2 case the inner disc does not perfectly align with the hole, as would be predicted by SF. This is due to the viscous inward advection of angular momentum from the outer disc (neglected in the analysis by SF [cf their Equation (6) and the following approximations]. This term scales as ν_1/ν_2 and indeed the misalignment at small radii disappears in the right panel in Fig. 1, where $\nu_1/\nu_2 = 0.1$.

An important quantity to be evaluated is the torque $\mathbf{T} = {\rm d}\mathbf{J}_{\rm h}/{\rm d}t$ exerted on the hole by the disc. Note that, if we take the z-axis to be aligned with the hole's spin, the torque has only got the x and y components, which are proportional to the y and x components of the disc's angular momentum, respectively. Note that it is the x-component of the torque which is responsible for the alignment of the hole with the disc's angular momentum, while the y-component gives rise to a precession of the hole spin. In the SF steady state, the two components of the torque $\mathbf{T}_{\rm SF,0} = (T_{{\rm SF}x}, T_{{\rm SF}y})$ are equal to each other in magnitude and are given by:

$$T_{{\rm SF}x} = -T_{{\rm SF}y} = -\pi K \Sigma_\infty \sqrt{\omega_{\rm p}\nu_2 GM}, \quad (12)$$

where Σ_∞ is the (almost) constant surface density far from the inner edge of the disc. In our case, we have $\Sigma_\infty = 1/3\pi$ (see Eq. 11). In order to check on which time-scale the asymptotic values of the torques expressed in equation (12) are attained, we have computed the torques on the hole exerted by our disc in the case where $\nu_2/\nu_1 = 10$, for which our solution eventually approaches the SF solution. Note that the values expressed in equation (12) come from an integral over the disc surface, assumed to extend from $R = 0$ to infinity. For a disc extending from $R_{\rm in}$ to $R_{\rm out}$ the torque is given by:

$$\mathbf{T}_{\rm SF} = -2\pi \int_{R_{\rm in}}^{R_{\rm out}} \frac{\boldsymbol{\omega}_{\rm p} \times \mathbf{L}}{R^3} R{\rm d}R = C(R_{\rm in}, R_{\rm out})\mathbf{T}_{\rm SF,0}, \quad (13)$$

where $C(R_{\rm in}, R_{\rm out})$ is a correction factor of order unity, that can be easily computed analytically based on the SF solution [Eq. (7)].

Fig. 2 shows the evolution of the x- (left panel) and y- (right panel) components of the torque, normalized to the asymptotic value predicted on the basis of the SF solution, $T_{\rm SF}$. Initially, the disc is only inclined with respect to the hole and does not precess (l_y is initially zero), and therefore the x-component of the torque is also vanishing. In contrast, the y-component of the torque, dependent on the relative inclination and responsible for the precession of the hole, is much larger than the asymptotic value. As the evolution proceeds, the disc acquires a non-vanishing l_y and starts to exert an aligning torque, T_x, on the hole. This reaches a maximum of $\approx 1.5 T_{\rm SF}$ at $t \approx 0.05$, and then slowly decreases, approaching the asymptotic value. Note that the value of T_x is never very far from the estimate of SF, which implies that the time-scale given by SF for the alignment of the hole is roughly correct. On the other hand, the component T_y of the torque is significantly different than the SF solution and approaches it much more slowly. This means that we expect the hole spin to precess at a significantly different and apparently faster rate.

3.2 Small warp radius

Here we describe the evolution of the system with a smaller warp radius $R_{\rm w} = 2.5R_{\rm in}$. The ratio of the two viscosities is here taken to be $\nu_2/\nu_1 = 10$. The initial inclination angle between the disc and the hole was here taken to be $\theta = 0.05$. Fig. 3 describes the evolution of the relative inclination between the hole and the disc with time. The solid line refers to $t = 0.5$, the short-dashed line to $t = 3$, while the long-dashed line refers to $t = 60$ (in units of the viscous time-scale at $R = 1$). The disc in this case eventually approaches a steady state, but this is significantly different than what predicted by SF (shown in Fig. 3 with a dot-dashed line). This is to be expected, since their solution is only valid when the warp radius is much greater than the inner disc radius. Because the warp radius is not much larger than the inner disc radius, the inner disc is flat, but remains misaligned with the angular momentum of the hole.

4 WARPED SPREADING RINGS

From the discussion of previous section, it appears that an initially flat disc approaches the steady-state warped configuration rather slowly, on a time scale $t_{\nu_2} = R^2/\nu_2$. The surface density of the disc, on the other hand, evolves on the viscous time scale $t_{\nu_1} = R^2/\nu_1$. The ratio of the two time scales is $t_{\nu_2}/t_{\nu_1} = \nu_1/\nu_2$. Based on the linear calculations by Papaloizou & Pringle (1983), this ratio is small and the warped configuration can be achieved before the disc is accreted. However, especially for large warps, the linear calculations are expected to break down and the two time scales

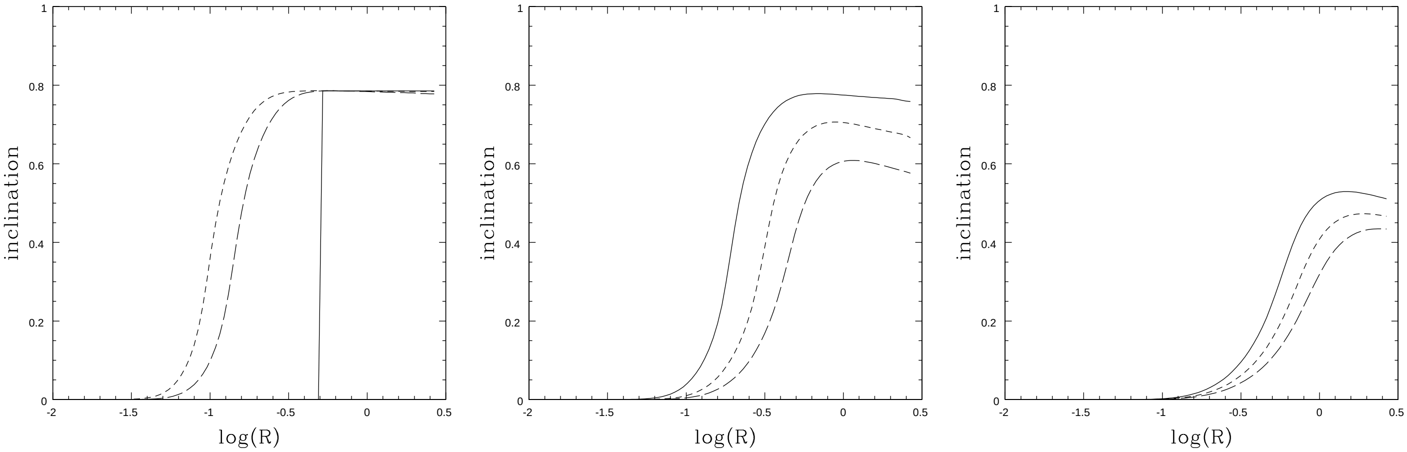

Figure 4. Evolution of the angle between the direction of $\mathbf{l}(R)$ (the local direction of the disc specific angular momentum) and that of the black hole angular momentum $\mathbf{J}_{\rm h}$, at different times during the evolution, for the case $\log R_{\rm w} = 0.3$ and $J_{\rm d} = J_{\rm h}$ (Note that throughout the paper we only plot the relative inclination between the disc and the hole in regions where the disc surface density is not negligible). Left panel: the lines refer to $t = 0$ (solid line), $t = 3 \times 10^{-3}$ (short-dashed line) and 6×10^{-3} (long-dashed line). Middle panel: the lines refer to $t = 0.01$ (solid line), $t = 0.02$ (short-dashed line) and $t = 0.03$ (long-dashed line). Right panel: the lines refer to $t = 0.04$ (solid line), $t = 0.05$ (short-dashed line) and $t = 0.06$ (long-dashed line). At $t = 0$ the matter is in a ring at $\log R = 0$. By $t \approx 0.3$ the whole disc has aligned with the hole spin.

might even become comparable. It might then be questionable whether the SF solution can be actually attained in realistic systems.

In reality, as we have mentioned, the surface density profile of the disc is unlikely to be that of a steady disc. In practice what we wish to model is an accretion event (or a succession of events) onto the central black hole in a galactic nucleus. Such events appear to occur at random orientations relative to the black hole spin. For this reason, in order to examine more carefully the dynamical evolution of a warped disc under relatively more realistic configurations, we have performed a number of other simulations, where we evolve a system initially comprising a thin ring of matter orbiting around a black hole whose spin is misaligned with the direction of the ring rotation. These simulations have also the advantage of having a well defined total disc angular momentum. In this case, we also allow the hole spin to evolve according to equation (6). In this case, we can use a slightly smaller dynamical range, since throughout the simulations the ring never spreads outside $R = 5$. Therefore, the grid in this case extends from $R = 10^{-2}$ to $R = 5$ for most simulations. In a couple of cases however (when we consider small warp radii, see below section 4.2) the inner radius was decreased to $R_{\rm in} = 5 \times 10^{-3}$, in order for it to be significantly smaller than the warp radius. We initialize the simulations by setting up a thin ring of matter, with a Gaussian surface density profile, centered around $R_0 = 1$ and with an initial width equal to $\Delta R = 10^{-2}$. The disc is initially flat and inclined by an angle θ with respect to the hole spin. The modulus of the angular momentum of the disc is therefore $J_{\rm d} = M_{\rm d}\sqrt{GMR_0}$ (where $M_{\rm d}$ is the total disc mass). The governing equations only depend on the parameters ν_2/ν_1, $J_{\rm h}/J_{\rm d}$, and on the ratio $R_{\rm w}/R_0$. We have performed a number of different simulations by varying the parameters above. In the following we will describe in more detail the behaviour of the system for a number of different initial configurations.

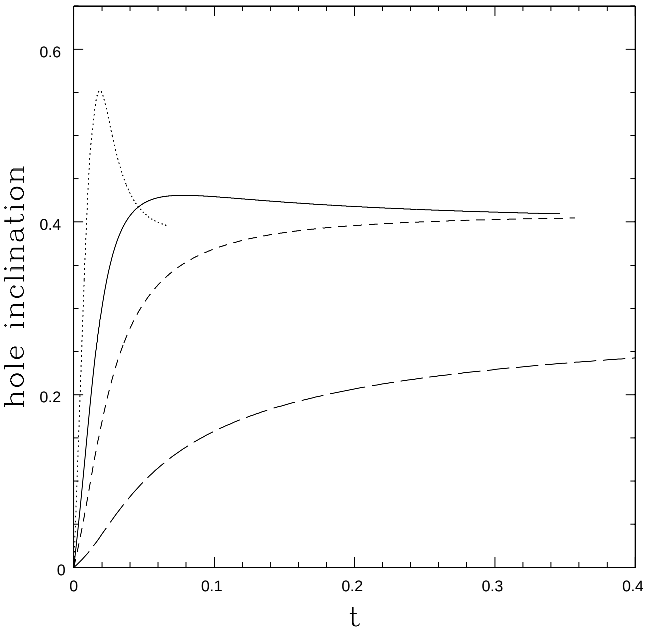

Figure 5. Evolution of the angle between the hole spin and the z-axis for the case $J_{\rm d} = J_{\rm h}$ and $R_{\rm w}/R_0 = 2$. If angular momentum is conserved, and if the systems becomes eventually completely aligned, we would expect the final inclination to be $\phi \approx 0.4$. The lines refer to $\nu_2/\nu_1 = 30, 10, 5$ and 1 (dotted, solid, short-dashed and long-dashed lines, respectively).

4.1 Alignment

In this case, we take $R_{\rm w} = 2R_0 = 200R_{\rm in}$ (so that the initial material is deposited just outside the warp radius) and $\nu_2/\nu_1 = 10$. We also take the initial relative inclination to be $\theta = \pi/4$ and the ratio of angular momenta to be $J_{\rm d}/J_{\rm h} = 1$.

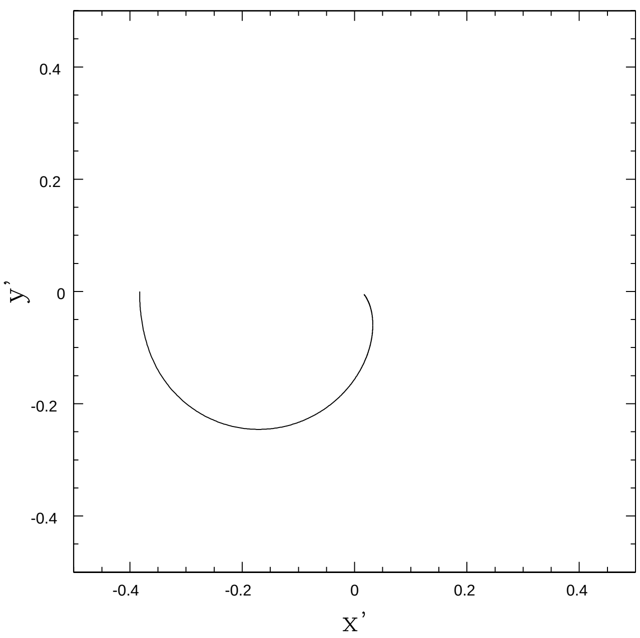

Figure 6. The case $J_{\rm d} = J_{\rm h}$, $R_{\rm w}/R_0 = 2$ and $\nu_2 = 10\nu_1$. Evolution of the tip of the unit vector parallel to the black hole spin instantaneous direction in the (x', y') plane, perpendicular to the direction of the total angular momentum of the system $\mathbf{J}_{\rm h} + \mathbf{J}_{\rm d}$. The hole aligns after roughly half a turn in this plane, showing that the precession time-scale is of the same order of the alignment time-scale.

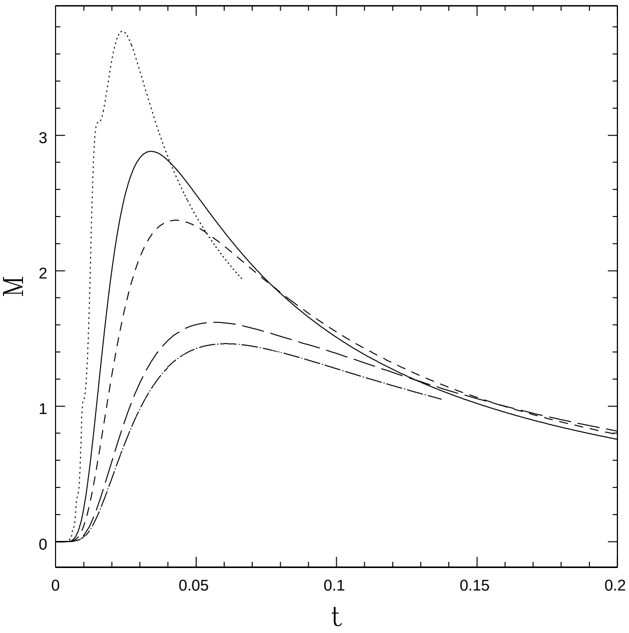

Figure 7. The case $J_{\rm d} = J_{\rm h}$, $R_{\rm w}/R_0 = 2$. Evolution of the mass accretion rate on the hole in the cases where $\nu_2/\nu_1 = 30, 10, 5$ and 1 (dotted, solid, short-dashed and long-dashed line, respectively), and in the case of a flat spreading ring (dot-dashed line). The twisting of the disc and the mixing of angular momenta between different radii increases the accretion rate by as much as a factor of 3-4.

In this case, the condition expressed in inequality (1) would tell us that we expect the disc and the hole to align.

The evolution of the relative inclination of the disc and the hole is shown in Fig. 4. The plots display the angle between the local direction of the disc specific angular momentum $\mathbf{l}$ and the direction of the hole angular momentum, as a function of radius R, at different times during the evolution (see caption for details), expressed in units of the viscous time-scale at $R = R_0$, $t_0 = R_0^2/\nu_1$. At $t = 0$ the disc is flat and confined in a narrow ring, but then, as it spreads to smaller radii, it also gets warped and the inner disc tends to become aligned with the hole. By the time $t \approx 0.3t_0$, most of the disc has aligned with the hole. This is consistent with the propagation of the warp being roughly a factor $\nu_2/\nu_1 = 10$ faster than the spreading of the ring.

The solid line in Fig. 5 shows the evolution of the angle between the hole spin and the z-axis (which coincides with the initial direction of the hole spin). During the evolution of the system, angular momentum is not perfectly conserved, because mass (and correspondingly angular momentum) is being removed from the inner disc, to allow for accretion. However, the angular momentum removed in this way is, in general, a small fraction of the total angular momentum, since the specific angular momentum in the inner disc is a factor $\sqrt{R_{\rm in}/R_0} \sim 0.1$ smaller than the total. Neglecting this contribution and assuming that the total angular momentum of the system $\mathbf{J}_{\rm h} + \mathbf{J}_{\rm d}$ is conserved, we can get a simple relationship between the final direction of the hole spin and the initial relative misalignment. In fact, if the system becomes eventually completely aligned, all components of the angular momentum should align with the direction of the total angular momentum (which is conserved). We then get that the angle ϕ between the initial and final direction of the hole spin is given by:

$$\cos\phi = \frac{1+\xi\cos\theta}{\sqrt{1+\xi^2+2\xi\cos\theta}}, \qquad (14)$$

where $\xi = J_{\rm d}/J_{\rm h}$. In the present case, where $\xi = 1$ and $\theta = \pi/4$, we expect $\phi \approx 0.4$, in agreement with the result shown in Fig. 5.

During the alignment process, the effect of the torques between the hole and the disc is not only to align the relative angular momenta, but, as discussed above, also to produce a precession of both the angular momentum of different annuli in the disc and of the spin of the black hole. In order to illustrate this, we plot in Fig. 6 the evolution of the tip of the unit vector parallel to the instantaneous direction of the black hole spin in a plane (x', y') perpendicular to the (constant) direction of the total angular momentum of the system. At the end of the alignment process, the hole spin should be parallel to the total angular momentum and the tip should therefore tend to become very close to the origin of this plane. This is indeed the behaviour shown in Fig. 6. The hole spin starts with a relatively large x component (it starts on the left in this plot) and, after roughly half a turn in this plane, eventually aligns with the total angular momentum. This also shows that the precession time-scale is of the same order as the alignment time-scale in agreement with the conclusion of SF.

The solid line in Fig. 7 shows the evolution of the mass

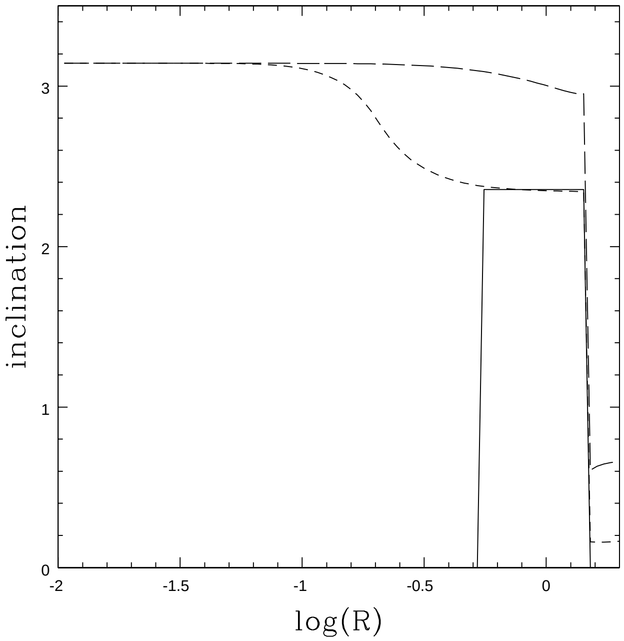

Figure 8. Evolution of the angle between $\mathbf{l}(R)$ and $\mathbf{J}_{\rm h}$ in the case where initially $\theta = 3\pi/4$ and $J_{\rm d}/J_{\rm h} = 1$, $\log R_{\rm w} = 0.3$ and $\nu_2/\nu_1 = 10$. The system eventually becomes counter-aligned The lines refer to times t =0, 0.01 and 0.1 in units of R_0^2/ν_1.

accretion rate with time. As we can see, the presence of the warp results in an enhancement of the mass accretion rate by as much as a factor 3, with respect to a non-warped spreading ring calculation (analogous to the standard case discussed by Pringle 1981), here shown with a dot-dashed line. This is due to the fact that the term associated with ν_2 induces some energy dissipation in the disc, which then is driven more efficiently to small radii. This process was already noted and described by Pringle (1992).

In order to illustrate how the behaviour of the disc changes when different values of ν_2/ν_1 are used, we have also run a number of simulations, identical to the previous one, but with $\nu_2/\nu_1 = 30$, $\nu_2/\nu_1 = 5$ and $\nu_2/\nu_1 = 1$. In actual discs, the ratio ν_2/ν_1 might be even larger than our largest value, but we expect that the trends derived here will hold also for even more extreme viscosity ratios.

The results of these other simulations are also shown in Fig. 5 and 7, where the dotted line refers to $\nu_2/\nu_1 = 30$, the short-dashed line to $\nu_2/\nu_1 = 5$ and the long-dashed line to $\nu_2/\nu_1 = 1$.

The results shown in Fig. 5 can be easily understood in terms of Eqs. (8) and (9), according to which the alignment timescale is inversely proportional to ν_2/ν_1. Indeed, when a large ν_2/ν_1 the disc and the hole rapidly get aligned between each other. An interesting feature appearing in the high ν_2/ν_1 simulations is that the hole inclination overshoots somewhat before settling down at the asymptotic value.

For what concerns the mass accretion rates, as expected, the increase in accretion when a warp is present is larger for larger values of ν_2/ν_1, consistent with our interpretation that it is the enhanced dissipation associated with ν_2 that drives most of the accretion process. However, note that the enhanced accretion does not scale linearly with ν_2/ν_1.

4.2 Counter-alignment

As a second test, we have considered the case where, as before, $R_{\rm warp} = 2R_0$, $\nu_2/\nu_1 = 10$ and $J_{\rm d}/J_{\rm h} = 1$. In this case, however, we start from initially almost anti-parallel angular momenta, with $\theta = 3\pi/4$. In this case King et al. (2005) predict that the disc and hole end-up counter-aligned, since in this case $J_{\rm d}/J_{\rm h} = 1 < -2\cos\theta \approx 1.41$. The evolution of the relative inclination of the disc and the hole is shown in Fig. 8. The three lines refer to $t = 0$ (solid line), $t = 0.01$ (short-dashed line) and $t = 0.1$ (long-dashed line). As can be seen the spreading of the ring is accompanied by a fast counter-alignment of the system (the angle approaching π), in agreement with King et al. (2005).

4.3 Eventual alignment with initial spins almost anti-parallel

As we have seen in the previous Section, during the spreading of a ring of matter towards the black hole, when the initial angular momenta are almost anti-parallel, the inner part of the disc becomes rapidly counter-aligned with the spin of the hole. In general, the angular momentum of the part of the disc that first interacts with the hole is only a small fraction of the total. Therefore if the disc and hole are initially close to counter-alignment we would expect that this material would always counter-align, regardless of the total angular momentum of the disc. However, as noted by King et al. (2005), when the disc angular momentum is large, we should expect that eventually the system would tend to alignment. This brings the question of how this eventual alignment takes place, when initially the inner disc is expected to be counter-aligned. In order to answer to this question, we have performed another simulation, with the following parameters: $R_{\rm w} = 2R_0$, $\nu_2/\nu_1 = 10$ and $\theta = 3\pi/4$. This is similar to the case discussed above. However, we now take $J_{\rm d}/J_{\rm h} = 5$. In this case, $J_{\rm d}/J_{\rm h} = 5 > -2\cos\theta \approx 1.41$, and, according to King et al. (2005), we should have eventual alignment.

The evolution of the system is shown in Fig. 9. The left panels show the evolution of the relative inclination between the disc and the hole, while the right panels show the corresponding surface density of the disc. As can be seen the initial spreading is indeed accompanied by an counter-alignment (top panels). Note the effect of the enhanced dissipation due to the warp in the evolution of the surface density. In this case more matter flows in with respect to a non-warped spreading ring, resulting in a secondary "bump" at small radii in the surface density (compare with Fig. 3 of Pringle 1992, which shows the same effect, but for a smaller warp amplitude, and with Fig. 2 of Pringle 1981, which shows the evolution of a non-warped disc). The middle panels show the evolution at later stages. The disc has essentially broken into two: an inner counter-aligned disc and an outer disc, containing most of the disc angular momentum, with respect to which the system composed of black hole and inner disc tends progressively to align. The inner disc becomes smaller in size as time goes by, due to accretion (enhanced by the warping) and due to the fact that the inner disc is essentially disconnected from the outer disc. The bottom plots show the later evolution of the system. The inner disc is progressively accreted, while the outer disc becomes

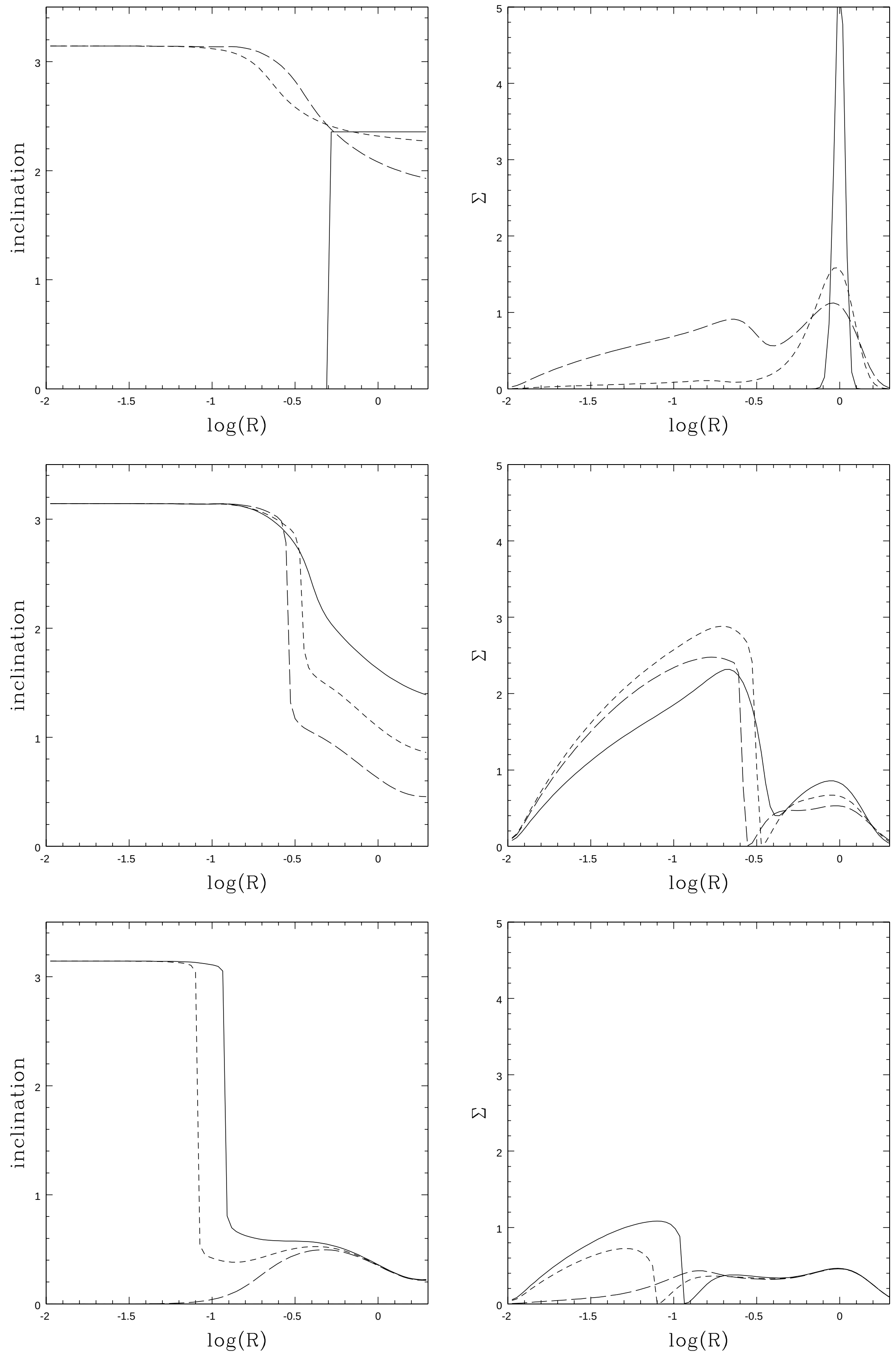

Figure 9. **Left**: Angle between $\mathbf{l}(R)$ and $\mathbf{J}_{\rm h}$ at various times during the evolution of a simulation where $J_{\rm d}/J_{\rm h} = 5$ and where the initial misalignment is $\theta = 3\pi/4$. Here $\log R_{\rm w} = 0.3$ and $\nu_2/\nu_1 = 10$. Top panel : at $t = 0$ (solid line), $t = 0.01$ (short-dashed line), $t = 0.02$ (long-dashed line). Middle panel: at $t = 0.03$ (solid line), $t = 0.04$ (short-dashed line) and $t = 0.05$ (long-dashed line). Bottom panel: at $t = 0.0568$ (solid line), $t = 0.0572$ (short-dashed line) and $t = 0.0576$ (long-dashed line). Time is in units of R_0^2/ν_1, where the ring is initially at $R_0 = 1$. **Right**: Corresponding surface densities of the disc.

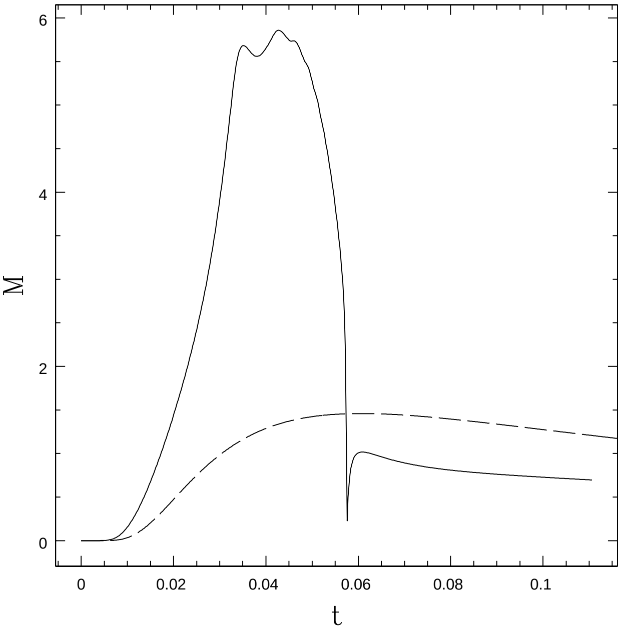

Figure 10. Evolution of the mass accretion rate onto the black hole for the case shown in Figure 9 where initially almost anti-parallel angular momenta eventually align. The dashed line shows the corresponding evolution for a flat spreading ring. The accretion rate is greatly enhanced during the accretion of the inner disc.

progressively more aligned with the hole. The long-dashed line in the bottom plots shows the final stage of the evolution, where the inner disc has been completely accreted and we are left with an aligned disc. The outer parts of the disc, which still have a small inclination with respect to the hole, are going to be aligned more slowly, due to the longer time-scales in the outer disc. We then see that the prediction by King et al. (2005) is still valid in this case.

The evolution of the mass accretion rate onto the hole is displayed in Fig. 10 with a solid line, while the dashed line shows the corresponding evolution for a flat disc. In this case, the strong warping produced in the initial counter-aligned configuration leads to a strong enhancement of the accretion rate, by factor ≈ 6. The accretion rate then suddenly drops when the inner disc has been completely accreted and then rises again to values of order unity as the final accretion of the outer disc takes place. During the first burst of accretion, roughly 20% of the disc mass is accreted.

Figure 11 shows the evolution of the tip of the unit vector parallel to the hole spin in the (x',y') plane, perpendicular to the direction of the total angular momentum $\mathbf{J}_{\rm t}$. In this case, the initial angle between $\mathbf{J}_{\rm h}$ and $\mathbf{J}_{\rm t}$ is larger than $\pi/2$, even though at later stages the two vectors eventually align. In Fig. 11 we display with a dotted line the early evolution of the spin direction, during which it has an angle larger than $\pi/2$ with respect to $\mathbf{J}_{\rm t}$, and with a solid line the later evolution, when the relative angle is smaller than $\pi/2$. The hole spin makes a full turn in this plane, showing that also in this case the precession rate is comparable to the alignment rate. In the course of the alignment the black hole spin axis traces out a large arc on the sky.

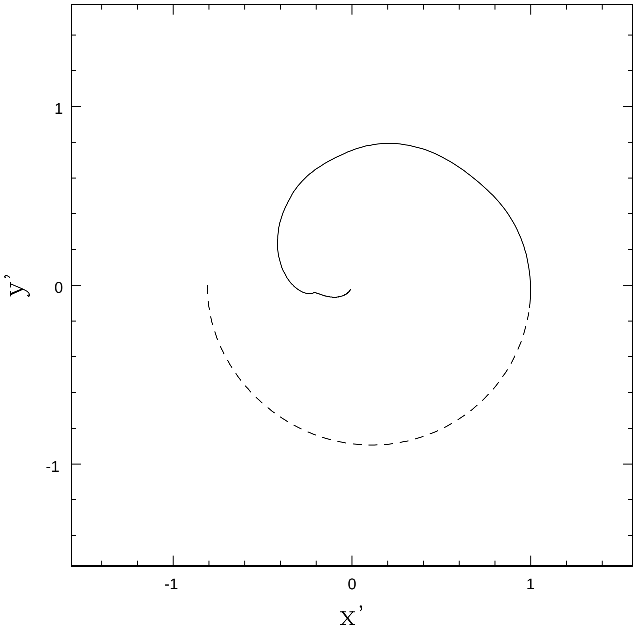

Figure 11. Evolution of the tip of the unit vector parallel to the black hole spin instantaneous direction in the (x',y') plane, perpendicular to the direction of the total angular momentum of the system $\mathbf{J}_{\rm h}+\mathbf{J}_{\rm d}$, in the case where the initial angular momentum of the hole is almost anti-parallel with respect to the disc's one and where $J_{\rm d}/J_{\rm h}=5$ (for details see Figure 9). In this case, the hole initially forms an angle larger than $\pi/2$ with $\mathbf{J}_{\rm t}$. The evolution is shown with a dotted line while the angle between $\mathbf{J}_{\rm h}$ and $\mathbf{J}_{\rm t}$ is larger than $\pi/2$, and with a solid line otherwise. Also in this case, the precession time-scale is of the same order of the alignment time-scale and the alignment takes place after roughly one full precession. Note that the black hole spin axis traces out a large arc on the sky.

4.4 Dependence on warp radius

One important parameter in the dynamics of the system considered here is the relative location of the warp radius $R_{\rm w}$ with respect to the radius within which most of the disc angular momentum resides, here identified with R_0. It is not simple to estimate the relative location of these two scales for realistic models of AGN discs. If we take a typical AGN model, such as the one by Collin-Souffrin & Dumont (1990) (see also King et al. 2005), we find that for a typical choice of parameters the radius at which the disc angular momentum equals the angular momentum of the hole is a few times the warp radius. However, one should keep in mind that these estimates are based on steady-state models of AGN discs, which might not be applicable on the time-scales considered here (and are certainly not appropriate in our spreading ring calculations).

In order to check the effect of the warp radius on the alignment process, we have performed a number of other simulations, similar to those presented above, but with different warp radius. In this cases, we have always taken $\nu_2/\nu_1=10$.

First, we considered the case where the initial inclination is $\theta=\pi/4$ and $J_{\rm d}/J_{\rm h}=1$, in which case we would expect the disc to align with the black hole (see section 4.1).

However, differently than what discussed in section 4.1, we take here $R_{\rm w} = 0.25R_0$, so that the ring is initially completely outside the warp radius. Figure 12 shows the evolution of hole inclination (left) and mass accretion rate (right) for this case. The dotted lines show the respective results for the analogous case with a large warp radius, described above in section 4.1. It can be seen that the time-scale for the alignment of the hole is longer in the case where the warp radius is smaller, in agreement with equation (9). The peak mass accretion rate on the hole is smaller in this case, with respect to the case with a larger warp radius.

Secondly, we considered the case where the initial inclination is $\theta = 3\pi/4$, $J_{\rm d}/J_{\rm h} = 1$ and $R_{\rm w} = 0.25R_0$. In this case, see section 4.2, we expect the disc and the hole to counter-align. Also this case does not present significant differences with respect to the case with a larger warp radius. The disc and the hole counter-align with respect to each other. Again, with a smaller warp radius the alignment time-scale is longer, as already noted above.

Thirdly, we considered the more interesting case where initially almost anti-parallel spins end up aligned. This could be a typical situation in many AGN. We have seen in the previous Section that in this case, initially the low angular momentum material that first arrives close to the hole tend to counter-align with the hole but then, after the accretion of this inner counter-aligned disc, the hole and the outer disc eventually align. We have performed a number of simulations in order to check the dependence of the time spent accreting in a counter-aligned fashion on the choice of the warp radius $R_{\rm w}$. In all these cases the initial inclination is $\theta = 3\pi/4$ and $\nu_2/\nu_1 = 10$, but the disc angular momentum is chosen so as to dominate on the hole, $J_{\rm d}/J_{\rm h} = 5$. We have then run a number of simulations with different $R_{\rm w}/R_0 = 0.25$, 0.1 and 0.05. In the last two cases, we have decreased the inner disc radius to $R_{\rm in} = 5\times 10^{-3}R_0$, in order for it to be significantly smaller than the warp radius. Fig. 13 shows the inclination of the inner disc relative to the hole as a function of time for the simulation where $R_{\rm w}/R_0 = 0.05$ (solid line), 0.1 (dotted line), 0.25 (short-dashed line) and 2 (long-dashed line). It can be seen that in all cases the systems switches from a counter-aligned to an aligned configuration, the transition (corresponding to the accretion of the inner disc, see previous Section) being progressively more gentle as the warp radius decreases. This is because, when $R_{\rm w}$ is smaller, the alignment between the hole and the outer disc is slower [see Eq. (9)], so that when the inner disc is accreted, the outer disc and the hole are still not aligned. As the warp radius decreases, the time spent accreting in an counter-aligned fashion increases and it can be a significant fraction of the accretion time-scale, up to $t \approx 0.2t_{\nu_1}(R_0)$, where $t_{\nu_1}(R_0)$ is the viscous time at $R = R_0$. This behaviour can be understood qualitatively in the following way. We expect that the transition between the counter-aligned and the aligned configuration occurs roughly when the angular momentum accreted through $R_{\rm w}$ becomes comparable with that of the hole [cf. Eq. (8)]. Since the specific angular momentum scales as $R^{1/2}$, in the case where $R_{\rm w}$ is smaller, a larger amount of matter needs to be accreted before the accreted angular momentum becomes comparable to that of the hole, so that the transition consequently occurs later. Equivalently, the same conclusion can be obtained if one considers that the alignment time-scale increases with decreasing $R_{\rm w}$ [Eq. (9)].

5 DISCUSSION AND CONCLUSIONS

In this paper we have considered the evolution of a system comprising an accretion disc and a central spinning black hole, in the case where the hole spin is misaligned with the rotation direction of the disc, and the disc is therefore subject to Lense-Thirring precession and becomes twisted and warped. Our approach is similar to the one considered by Pringle (1992), in that we consider the case where the warp propagates in the disc in a diffusive manner. However, while Pringle (1992) considered the warping of an otherwise steady-state disc, here we also consider the case where the surface density of the disc evolves as the disc is being warped. Furthermore, in our evolution scheme, the direction of the spin of the hole is allowed to move under the influence of the torques exerted by the disc.

We have carried out a series of simulations under different conditions. First, we have considered the warping of a disc which is initially characterized by a steady-state surface density distribution (Pringle 1992) and where the direction of the hole spin is kept fixed and considered various cases, where the location of the warp radius $R_{\rm w}$ and the ratio of the two viscosities ν_2/ν_1 are changed. We find that the disc eventually settles down in a steady warped configuration (similar to the one obtained analytically by SF), but this occurs over the relatively long time-scale associated with the warp propagation time-scale $t_{\nu_2} \approx R^2/\nu_2$, that can be a significant fraction of the accretion time-scale. We find that if the warp radius is small and the ratio of the two viscosities is of order unity, at small radii the warp structure can be significantly different from that predicted by SF.

We also find that the time-scale on which the black hole spin and the disc align can be comparable with the propagation time for the warp. We therefore also considered the probably more realistic situation in which a ring of matter is accreted by the hole (as can happen, for example, during an accretion event onto a central black hole in a galactic nucleus). As the ring spreads, it becomes warped and the direction of the hole spin is modified. A general feature of these warped spreading ring simulations is that the dissipation associated with the twisting of the disc leads to an enhanced accretion rate onto the hole (by as much as a factor 10).

We have computed the detailed evolution of the direction of the spin of the hole during the accretion and alignment process. We have found, in agreement with SF, that the "precession" time-scale (i.e. the time-scale of the change of the direction of the spin perpendicular to the total angular momentum) is comparable to the alignment time-scale, so that during alignment the spin of the hole only "goes round" at most once (see Figs. 7 and 11). If the jets emanating from AGN point in the instantaneous direction of the hole spin, our conclusions have important consequences on the shape of the observed "precessing" jets in these systems. Recently, Lister et al. (2003) have reported observations of a "precessing" jet most likely emanating from an AGN. They have fitted the shape of the observed jet by using a model where the nozzle precesses slowly around a fixed axis. However, if

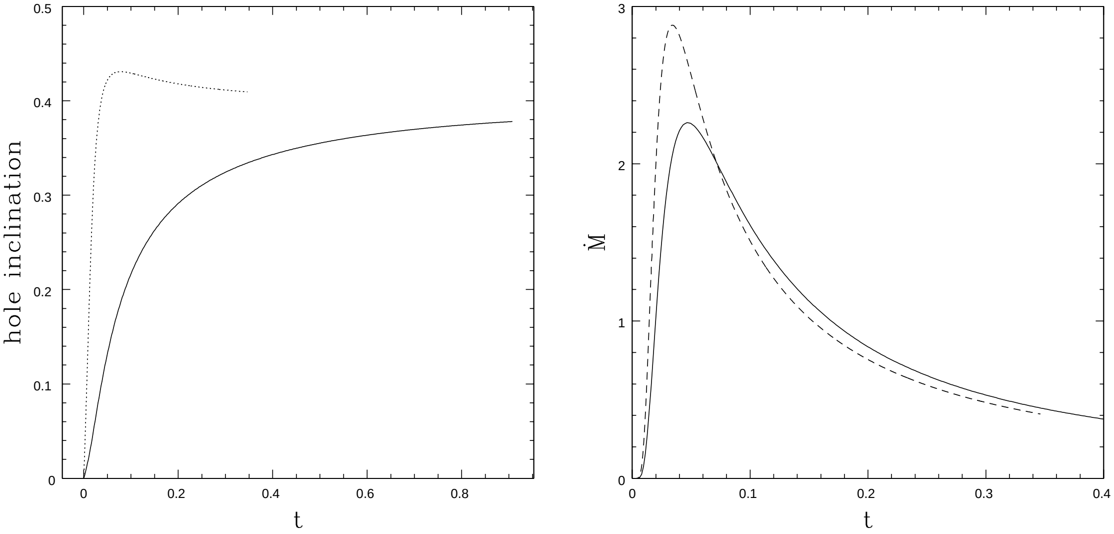

Figure 12. Left: Evolution of the inclination of the hole spin in the case where the initial misalignment is $\theta = \pi/4$, $J_{\rm d}/J_{\rm h} = 1$ and $R_{\rm w} = 0.25R_0$ (solid line) and $R_{\rm w} = 2R_0$ (dashed line). In the small warp radius case, the evolution of the hole spin is slower [cf. equation (9)]. **Right**: Mass accretion rate on the hole for the two cases.

the perturbation of the axis of the nozzle is indeed due to changes in the spin orientation of the black hole induced by the Bardeen-Petterson effect, then our results indicate that the assumption of precession around a fixed axis might not be correct. On the other hand, Lister et al. (2003) estimate that the typical length-scale of the jet is ≈ 280 pc, and that the advance speed of the lobes is $\approx 0.3c$. This would imply a "precession" time-scale of ≈ 3000 yrs, which is too small to be attributed to the Bardeen-Petterson effect [cf. our Eq. (9)]. In this particular case, the precession is more likely to result from spin-orbit coupling in a binary black hole system.

We would like to stress that the conclusion that alignment time-scale and "precession" time-scale are of the same order for the Bardeen-Petterson effect implies that (*i*) if proper precession around a fixed axis is observed, then it is most likely not due to Bardeen-Petterson alignment between the disc and the black hole and (*ii*) it provides an observational tool to estimate the alignment time-scale, by looking at the "precession" time-scale, for those systems where we are indeed looking at the Bardeen-Petterson effect.

We have also considered in detail the issue of the conditions under which the disc and the hole can be counter-aligned. We have confirmed the suggestion by King et al. (2005) that, if the initial misalignment between the disc and the hole is larger than 90 degrees and the hole angular momentum dominates the system, accretion proceeds in a counter-aligned fashion. However, also in the case where the disc angular momentum dominates and eventual alignment occurs, a large fraction of the mass is initially accreted in a counter-aligned fashion. We have shown (see Fig. 13) that the amount of time spent accreting in a counter-aligned fashion increases as the warp radius decreases. Indeed, the alignment time-scale [cf. Eq. (9)] scales as $R_{\rm w}^{-1/2}$. In a typical AGN, the alignment time-scale can be obtained combining our equation (9) with Eq. (22) of King et al. (2005) (to estimate $R_{\rm w}/R_{\rm S}$). This gives:

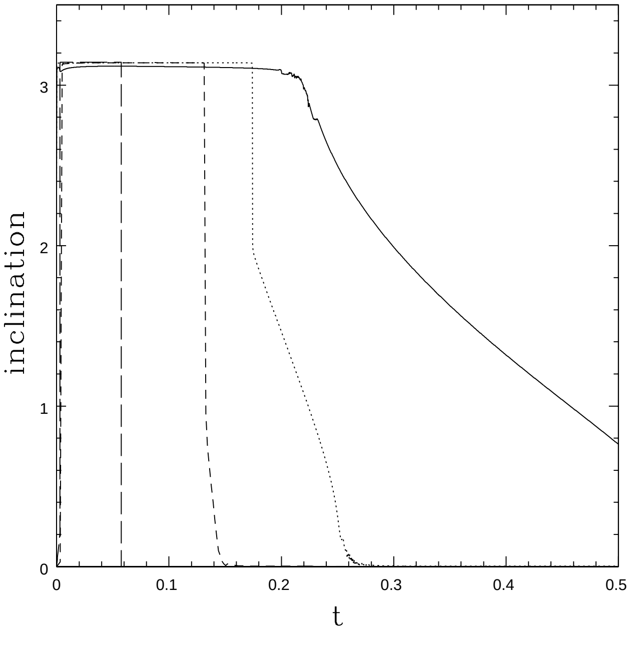

Figure 13. Inclination between the inner disc and the hole as a function of time (in units of the viscous time-scale R^2/ν_1 at $R = R_0$ for the cases where the initial spins are almost anti-parallel, the angular momentum ratio is $J_{\rm d}/J_{\rm h} = 5$ and $R_{\rm w}/R_0 = 0.05$ (solid line), 0.1 (dotted line), 0.25 (short-dashed line) and 2 (long-dashed line).

$$t_{\rm align} \approx 8.1 \times 10^6 a^{11/16} \left(\frac{\epsilon}{0.1}\right)^{7/8} \left(\frac{L}{0.1L_{\rm E}}\right)^{-7/8}$$

$$M_8^{-1/16} \left(\frac{\alpha_1}{0.03}\right)^{15/16} \left(\frac{\alpha_2}{0.3}\right)^{-11/16} {\rm yrs}, \qquad (15)$$

where ϵ is the efficiency of accretion, L is the AGN luminosity, $L_{\rm E}$ is the Eddington luminosity, M_8 is the black hole mass in units of $10^8 M_{\odot}$, and α_1 and α_2 are the α parameters corresponding to ν_1 and ν_2, respectively. We therefore see that the alignment time-scale is of the order of the lifetime of a typical AGN ($\approx 10^7$ yrs), and we might expect AGN to spend a relatively long time accreting in a counter-aligned fashion. This counter-aligned accretion mode can have important consequences on observables of AGN, such as the shape of X-ray iron lines, since for counter-aligned accretion the last stable orbit is at a significantly larger radius than for the aligned case.

However, we have also shown that the disc can suffer an abrupt change in orientation at a radius close to the warp radius, especially during counter-aligned accretion (see Figs. 4 and 9). A large fraction of the solid angle as seen from the center will be filled by the disc itself. This can lead to significant absorption of X-rays produced in the inner disc from the outer disc (Phinney 1989). The surface density of a steady-state AGN disc at $R_{\rm w}$ is (Collin-Souffrin & Dumont 1990):

$$\Sigma \approx 2.8\times 10^5 a^{-3/8}\left(\frac{\epsilon}{0.1}\right)^{-3/4}\left(\frac{L}{0.1L_{\rm E}}\right)^{3/4} M_8^{1/8} \left(\frac{\alpha_1}{0.03}\right)^{-7/8}\left(\frac{\alpha_2}{0.3}\right)^{3/8} {\rm g/cm^2}, \qquad (16)$$

which is high enough to obscure visibility of the central object. This implies that direct observation of counter-aligned accretion in observationally biased against, so that most of those AGN for which the central regions are visible are most likely to be co-rotating.

Our results are also relevant in order to determine the black hole spin history during the earlier phases (which appear to occur at redshift $1 < z < 5$) when the black hole acquires most of its mass. During this phase, each accretion event increases the black hole mass significantly ($\Delta M/M \sim 1-3$, Volonteri et al. 2005). In general, accretion of counter-aligned material spins the hole down. However, since the mass accreted during each event is of the order of the hole's mass, *if all the accreted material rotates about the same axis*, we would be in a situation like our Fig. 9 and the black hole would end up aligned and maximally spinning, as suggested by Volonteri et al. (2005). However, if this is not the case, we might regard one accretion event as a sequence of smaller accretion events where at every time the angular momentum of the accreted material is small compared to the hole. In such a situation, most of the accretion can occur in a counter-aligned way and the hole need not end up maximally rotating. Thus the result would be a spread of black hole spins (cf Fig. 8 in Volonteri et al. 2005). We conclude that the outcome for the spin history during this phase depends crucially on the details of the merging process.

We should mention that in our approach we have neglected the evolution of the magnitude of the spin of the hole as a consequence of accretion. This, however, is a small fraction of the total angular momentum of the system, since it scales approximately as $M_{\rm acc}R_{\rm in}^{1/2}$, where $M_{\rm acc}$ is the mass accreted by the hole and $R_{\rm in}$. We should also mention that in our simulations we have assumed that $R_{\rm in} = 0.005-0.01R_0$, where R_0 is the initial radius at which matter in injected. In actual AGN discs, the inner disc radius (which is of the order of the Schwarzschild radius) might be much smaller than this, but this does not affect our conclusions as long as $R_{\rm w}$ is much larger than $R_{\rm in}$.

A further important uncertainty in what we have described in this paper is the magnitude of the viscosity ν_2 associated with the propagation of the warp. This determines the location of the warp radius and the time-scale of the alignment process. Papaloizou & Pringle (1983) have shown that in the linear regime $\nu_2/\nu_1 = 1/2\alpha_1^2$, where α_1 is the standard viscosity parameter. However, it is not yet clear what would happen in the strongly non-linear case described here. Numerical simulations up to now have only addressed the case where the disc is relatively thick and warp propagation occurs in a wave-like manner (Nelson & Papaloizou 1999, 2000; Fragile & Anninos 2005). One possibility is that the flow becomes unstable (Gammie et al. 2000), such that perhaps $\nu_2 \approx \nu_1$. In some of the cases discussed here the disc can actually break in the sense that the tilt angle shows a sharp jump at some radius (see our Fig. 9, for example). In such conditions (see also the numerical simulations by Larwood et al. 1996) the diffusive equations adopted here might not be adequate. To resolve this issue we clearly need detailed numerical simulations of warp propagation in thin and viscous discs.

ACKNOWLEDGEMENTS

We thank Andrew King, Steve Lubow, Gordon Ogilvie, Martin Rees and Marta Volonteri for inspiring discussions and Cathie Clarke for a careful reading of the manuscript.

REFERENCES

Balbus S. A., Hawley J. F., 1998, Reviews of Modern Physics, 70, 1

Bardeen J. M., Petterson J. A., 1975, ApJ, 195, L65

Collin-Souffrin S., Dumont A. M., 1990, A&A, 229, 292

Fragile P. C., Anninos P., 2005, ApJ, 623, 347

Gammie C. F., Goodman J., Ogilvie G. I., 2000, MNRAS, 318, 1005

Greenhill L. J., Kondratko P. T., Lovell J. E. J., Kuiper T. B. H., Moran J. M., Jauncey D. L., Baines G. P., 2003, ApJ, 582, L11

Herrnstein J. R., Greenhill L. J., Moran J. M., 1996, ApJ, 468, L17

Kendall P., Magorrian J., Pringle J. E., 2003, MNRAS, 346, 1078

King A. R., Lubow S. H., Ogilvie G. I., Pringle J. E., 2005, MNRAS, in press

Kinney A. L., Schmitt H. R., Clarke C. J., Pringle J. E., Ulvestad J. S., Antonucci R. R. J., 2000, ApJ, 537, 152

Kumar S., Pringle J. E., 1985, MNRAS, 213, 435

Larwood J. D., Nelson R. P., Papaloizou J. C. B., Terquem C., 1996, MNRAS, 282, 597

Lister M. L., Kellermann K. I., Vermeulen R. C., Cohen M. H., Zensus J. A., Ros E., 2003, ApJ, 584, 135

Natarajan P., Pringle J. E., 1998, ApJ, 506, L97

Nayakshin S., 2005, MNRAS, 359, 545

Nelson R. P., Papaloizou J. C. B., 1999, MNRAS, 309, 929

Nelson R. P., Papaloizou J. C. B., 2000, MNRAS, 315, 570

Ogilvie G. I., 1999, MNRAS, 304, 557

Ogilvie G. I., 2000, MNRAS, 317, 607

Ogilvie G. I., Dubus G., 2001, MNRAS, 320, 485

Papaloizou J. C. B., Pringle J. E., 1983, MNRAS, 202, 1181
Phinney E. S., 1989, in NATO ASIC Proc. 290: Theory of Accretion Disks Dusty Disks and the Infrared Emission from AGN. p. 457
Pringle J. E., 1981, ARA&A, 19, 137
Pringle J. E., 1992, MNRAS, 258, 811
Pringle J. E., Verbunt F., Wade R. A., 1986, MNRAS, 221, 169
Rees M. J., 1978, Nature, 275, 516
Saitoh T. R., Wada K., 2004, ApJ, 615, L93
Scheuer P. A. G., Feiler R., 1996, MNRAS, 282, 291
Schmitt H. R., Pringle J. E., Clarke C. J., Kinney A. L., 2002, ApJ, 575, 150
Shakura N. I., Sunyaev R. A., 1973, A&A, 24, 337
Torkelsson U., Ogilvie G. I., Brandenburg A., Pringle J. E., Nordlund Å., Stein R. F., 2000, MNRAS, 318, 47
Volonteri M., Madau P., Quataert E., Rees M. J., 2005, ApJ, 620, 69
Wijers R. A. M. J., Pringle J. E., 1999, MNRAS, 308, 207